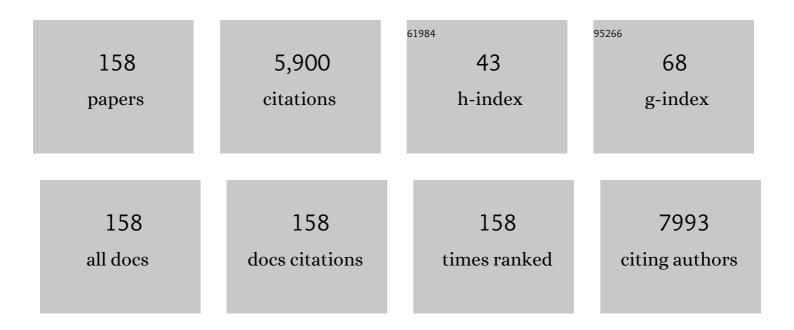
List of Publications by Year in descending order

Source: https://exaly.com/author-pdf/1987181/publications.pdf Version: 2024-02-01



VIIAN LIN

#	Article	IF	CITATIONS
1	Kinetics Tuning of Li-Ion Diffusion in Layered Li(Ni <sub><i>x</i></sub> Mn <sub><i>y</i></sub> Co <sub><i>z</i></sub> )O <sub>2</sub> . Journal of the American Chemical Society, 2015, 137, 8364-8367.	13.7	292
2	2H- and 1T- mixed phase few-layer MoS2 as a superior to Pt co-catalyst coated on TiO2 nanorod arrays for photocatalytic hydrogen evolution. Applied Catalysis B: Environmental, 2019, 241, 236-245.	20.2	242
3	Sn-Doped TiO <sub>2</sub> Photoanode for Dye-Sensitized Solar Cells. Journal of Physical Chemistry C, 2012, 116, 8888-8893.	3.1	241
4	Photovoltaic performance improvement of dye-sensitized solar cells based on tantalum-doped TiO2 thin films. Electrochimica Acta, 2010, 56, 396-400.	5.2	156
5	Mitoflash frequency in early adulthood predicts lifespan in Caenorhabditis elegans. Nature, 2014, 508, 128-132.	27.8	121
6	Phenothiazine–triphenylamine based organic dyes containing various conjugated linkers for efficient dye-sensitized solar cells. Journal of Materials Chemistry, 2012, 22, 25140.	6.7	120
7	Identification and characterization of alphavirus M1 as a selective oncolytic virus targeting ZAP-defective human cancers. Proceedings of the National Academy of Sciences of the United States of America, 2014, 111, E4504-12.	7.1	118
8	Fabrication of high performance Pt counter electrodes on conductive plastic substrate for flexible dye-sensitized solar cells. Electrochimica Acta, 2010, 55, 3721-3726.	5.2	116
9	Targeting oncogenic miR-335 inhibits growth and invasion of malignant astrocytoma cells. Molecular Cancer, 2011, 10, 59.	19.2	113
10	Light harvesting enhancement for dye-sensitized solar cells by novel anode containing cauliflower-like TiO2 spheres. Journal of Power Sources, 2008, 182, 370-376.	7.8	109
11	SAFE-clustering: Single-cell Aggregated (from Ensemble) clustering for single-cell RNA-seq data. Bioinformatics, 2019, 35, 1269-1277.	4.1	104
12	Room temperature fabrication of porous ZnO photoelectrodes for flexible dye-sensitized solar cells. Chemical Communications, 2007, , 2847.	4.1	97
13	An expanded landscape of human long noncoding RNA. Nucleic Acids Research, 2019, 47, 7842-7856.	14.5	92
14	Janus Solid–Liquid Interface Enabling Ultrahigh Charging and Discharging Rate for Advanced Lithium-Ion Batteries. Nano Letters, 2015, 15, 6102-6109.	9.1	90
15	An iodine-free electrolyte based on ionic liquid polymers for all-solid-state dye-sensitized solar cells. Chemical Communications, 2011, 47, 2700.	4.1	88
16	The Anti-Warburg Effect Elicited by the cAMP-PGC1α Pathway Drives Differentiation of Glioblastoma Cells into Astrocytes. Cell Reports, 2017, 18, 468-481.	6.4	85
17	Triphenylamine-based starburst dyes with carbazole and phenothiazine antennas for dye-sensitized solar cells. Journal of Power Sources, 2012, 199, 426-431.	7.8	83
18	Investigation of PEO-imidazole ionic liquid oligomer electrolytes for dye-sensitized solar cells. Solar Energy Materials and Solar Cells, 2007, 91, 785-790.	6.2	82

#	Article	IF	CITATIONS
19	Electrophoretic deposition of nanocrystalline TiO2 films on Ti substrates for use in flexible dye-sensitized solar cells. Electrochimica Acta, 2009, 54, 4467-4472.	5.2	80
20	Single-cell transcriptomic analysis in a mouse model deciphers cell transition states in the multistep development of esophageal cancer. Nature Communications, 2020, 11, 3715.	12.8	79
21	A 7.72% efficient dye sensitized solar cell based on novel necklace-like polymer gel electrolyte containing latent chemically cross-linked gel electrolyte precursors. Chemical Communications, 2005, , 5687.	4.1	73
22	Synthesis and ionic conductivity of a polysiloxane containing quaternary ammonium groups. Polymers for Advanced Technologies, 2004, 15, 61-64.	3.2	71
23	Facile Synthesis of Poly(3,4-ethylenedioxythiophene) Film via Solid-State Polymerization as High-Performance Pt-Free Counter Electrodes for Plastic Dye-Sensitized Solar Cells. ACS Applied Materials & Interfaces, 2013, 5, 8423-8429.	8.0	68
24	Prelithiation Activates Li(Ni <sub>0.5</sub> Mn <sub>0.3</sub> Co <sub>0.2</sub> )O <sub>2</sub> for High Capacity and Excellent Cycling Stability. Nano Letters, 2015, 15, 5590-5596.	9.1	68
25	Large-field high-resolution two-photon digital scanned light-sheet microscopy. Cell Research, 2015, 25, 254-257.	12.0	67
26	Enhanced performance of CdTe quantum dot sensitized solar cell via anion exchanges. Journal of Power Sources, 2015, 277, 215-221.	7.8	67
27	A novel high-performance counter electrode for dye-sensitized solar cells. Electrochimica Acta, 2005, 50, 5546-5552.	5.2	65
28	Improvements of photocurrent by using modified SiO2 in the poly(ether urethane)/poly(ethylene) Tj ETQq0 0 0 r 2009, , 3895.	gBT /Over 4.1	lock 10 Tf 50 62
29	High-Performance Plastic Platinized Counter Electrode <i>via</i> Photoplatinization Technique for Flexible Dye-Sensitized Solar Cells. ACS Nano, 2012, 6, 9596-9605.	14.6	62
30	Electrodeposition of Platinum on Plastic Substrates as Counter Electrodes for Flexible Dye-Sensitized Solar Cells. Journal of Physical Chemistry C, 2012, 116, 2850-2857.	3.1	62
31	Low temperature electrochemical deposition of nanoporous ZnO thin films as novel NO2 sensors. Electrochimica Acta, 2013, 90, 530-534.	5.2	59
32	Two-Step Electrochemical Synthesis of Polypyrrole/Reduced Graphene Oxide Composites as Efficient Pt-Free Counter Electrode for Plastic Dye-Sensitized Solar Cells. ACS Applied Materials & Interfaces, 2014, 6, 16249-16256.	8.0	59
33	Gel polymer electrolytes based on polyacrylonitrile and a novel quaternary ammonium salt for dye-sensitized solar cells. Materials Research Bulletin, 2004, 39, 2113-2118.	5.2	58
34	Solidification of liquid electrolyte with imidazole polymers for quasi-solid-state dye-sensitized solar cells. Materials Chemistry and Physics, 2008, 107, 61-66.	4.0	56
35	Targeting VCP enhances anticancer activity of oncolytic virus M1 in hepatocellular carcinoma. Science Translational Medicine, 2017, 9, .	12.4	55
36	Sonication–hydrothermal combination technique for the synthesis of titanate nanotubes from commercially available precursors. Materials Research Bulletin, 2006, 41, 237-243.	5.2	53

#	Article	IF	CITATIONS
37	The use of poly(vinylpyridine-co-acrylonitrile) in polymer electrolytes for quasi–solid dye-sensitized solar cells. Electrochimica Acta, 2007, 52, 4858-4863.	5.2	53
38	Enhancing the performance of dye-sensitized solar cells: doping SnO <sub>2</sub> photoanodes with Al to simultaneously improve conduction band and electron lifetime. Journal of Materials Chemistry A, 2015, 3, 3066-3073.	10.3	51
39	A new ionic liquid based quasi-solid state electrolyte for dye-sensitized solar cells. Journal of Photochemistry and Photobiology A: Chemistry, 2008, 194, 20-26.	3.9	50
40	Mn3O4/graphene composite as counter electrode in dye-sensitized solar cells. RSC Advances, 2014, 4, 15091.	3.6	50
41	Oncolytic Viro-Immunotherapy: An Emerging Option in the Treatment of Gliomas. Frontiers in Immunology, 2021, 12, 721830.	4.8	50
42	Improved photovoltaic performance of dye-sensitized solar cells (DSSCs) by Zn+Mg co-doped TiO2 electrode. Electrochimica Acta, 2013, 95, 48-53.	5.2	46
43	The effects of pyridine derivative additives on interface processes at nanocrystalline TiO <sub>2</sub> thin film in dyeâ€sensitized solar cells. Surface and Interface Analysis, 2007, 39, 809-816.	1.8	45
44	Improved photovoltaic performance of dye-sensitized solar cells by Sb-doped TiO2 photoanode. Electrochimica Acta, 2012, 77, 54-59.	5.2	45
45	Preparation of nanocrystalline TiO2 thin film at low temperature and its application in dye-sensitized solar cell. Journal of Solid State Electrochemistry, 2009, 13, 651-656.	2.5	43
46	Influence of the antennas in starburst triphenylamine-based organic dye-sensitized solar cells: phenothiazine versus carbazole. RSC Advances, 2012, 2, 4507.	3.6	43
47	Effects of different acceptors in phenothiazine-triphenylamine dyes on the optical, electrochemical, and photovoltaic properties. Dyes and Pigments, 2012, 94, 150-155.	3.7	43
48	Revealing the Relationship between Photocatalytic Properties and Structure Characteristics of TiO <sub>2</sub> Reduced by Hydrogen and Carbon Monoxide Treatment. ChemSusChem, 2018, 11, 2766-2775.	6.8	40
49	Influence of Sn source on the performance of dye-sensitized solar cells based on Sn-doped TiO2 photoanodes: A strategy for choosing an appropriate doping source. Electrochimica Acta, 2013, 107, 473-480.	5.2	39
50	Preparation and performance of dye-sensitized solar cells based on ZnO-modified TiO2 electrodes. International Journal of Minerals, Metallurgy and Materials, 2010, 17, 92-97.	4.9	38
51	In-situ photo-deposition CuO1â^ cluster on TiO2 for enhanced photocatalytic H2-production activity. International Journal of Hydrogen Energy, 2017, 42, 19942-19950.	7.1	38
52	DNA-PK inhibition synergizes with oncolytic virus M1 by inhibiting antiviral response and potentiating DNA damage. Nature Communications, 2018, 9, 4342.	12.8	38
53	Naturally Existing Oncolytic Virus M1 Is Nonpathogenic for the Nonhuman Primates After Multiple Rounds of Repeated Intravenous Injections. Human Gene Therapy, 2016, 27, 700-711.	2.7	37
54	Activation of Cyclic Adenosine Monophosphate Pathway Increases the Sensitivity of Cancer Cells to the Oncolytic Virus M1. Molecular Therapy, 2016, 24, 156-165.	8.2	35

#	Article	IF	CITATIONS
55	High-performance novel acidic ionic liquid polymer/ionic liquid composite polymer electrolyte for dye-sensitized solar cells. Electrochemistry Communications, 2011, 13, 60-63.	4.7	34
56	Selective replication of oncolytic virus M1 results in a bystander killing effect that is potentiated by Smac mimetics. Proceedings of the National Academy of Sciences of the United States of America, 2017, 114, 201701002.	7.1	33
57	Theoretical calculations and controllable synthesis of MoSe2/CdS-CdSe with highly active sites for photocatalytic hydrogen evolution. Chemical Engineering Journal, 2020, 383, 123133.	12.7	33
58	A novel polymer quaternary ammonium iodide and application in quasi-solid-state dye-sensitized solar cells. Journal of Photochemistry and Photobiology A: Chemistry, 2005, 170, 1-6.	3.9	32
59	Conversion enhancement of flexible dye-sensitized solar cells based on TiO2 nanotube arrays with TiO2 nanoparticles by electrophoretic deposition. Electrochimica Acta, 2011, 56, 6184-6188.	5.2	32
60	Novel organic dye employing dithiafulvenyl-substituted arylamine hybrid donor unit for dye-sensitized solar cells. Organic Electronics, 2013, 14, 2132-2138.	2.6	32
61	Intravenous injection of the oncolytic virus M1 awakens antitumor T cells and overcomes resistance to checkpoint blockade. Cell Death and Disease, 2020, 11, 1062.	6.3	32
62	Nitrogen-doped graphene as transparent counter electrode for efficient dye-sensitized solar cells. Materials Research Bulletin, 2012, 47, 4252-4256.	5.2	31
63	Cauliflower-like TiO2 rough spheres: Synthesis and applications in dye sensitized solar cells. Microporous and Mesoporous Materials, 2008, 112, 45-52.	4.4	30
64	Influence of VB group doped TiO2 on photovoltaic performance of dye-sensitized solar cells. Applied Surface Science, 2013, 277, 231-236.	6.1	30
65	Combining NanoKnife with M1 oncolytic virus enhances anticancer activity in pancreatic cancer. Cancer Letters, 2021, 502, 9-24.	7.2	30
66	X-ray photoelectron spectroscopy analysis of the stability of platinized catalytic electrodes in dye-sensitized solar cells. Surface and Interface Analysis, 2004, 36, 1437-1440.	1.8	29
67	Controllable synthesis of anatase TiO2 crystals for high-performance dye-sensitized solar cells. Journal of Materials Chemistry A, 2013, 1, 5347.	10.3	29
68	Novel organic sensitizers containing dithiafulvenyl units as additional donors for efficient dye-sensitized solar cells. RSC Advances, 2014, 4, 34896.	3.6	29
69	TiO2 compact layer for dye-sensitized SnO2 nanocrystalline thin film. Electrochimica Acta, 2014, 147, 366-370.	5.2	29
70	Metal and F dual-doping to synchronously improve electron transport rate and lifetime for TiO <sub>2</sub> photoanode to enhance dye-sensitized solar cells performances. Journal of Materials Chemistry A, 2015, 3, 5692-5700.	10.3	29
71	Cyclophilin D regulates mitochondrial flashes and metabolism in cardiac myocytes. Journal of Molecular and Cellular Cardiology, 2016, 91, 63-71.	1.9	29
72	Brain activity regulates loose coupling between mitochondrial and cytosolic Ca2+ transients. Nature Communications, 2019, 10, 5277.	12.8	29

#	Article	IF	CITATIONS
73	Influences of poly(ether urethane) introduction on poly(ethylene oxide) based polymer electrolyte for solvent-free dye-sensitized solar cells. Electrochimica Acta, 2009, 54, 6645-6650.	5.2	28
74	How to Optimize the Interface between Photosensitizers and TiO <sub>2</sub> Nanocrystals with Molecular Engineering to Enhance Performances of Dye-Sensitized Solar Cells?. ACS Applied Materials & Interfaces, 2015, 7, 25341-25351.	8.0	28
75	Intravenous injections of the oncolytic virus M1 as a novel therapy for muscle-invasive bladder cancer. Cell Death and Disease, 2018, 9, 274.	6.3	28
76	Rectification and tunneling effects enabled by Al2O3 atomic layer deposited on back contact of CdTe solar cells. Applied Physics Letters, 2015, 107, .	3.3	27
77	Triptolide inhibits proliferation and invasion of malignant glioma cells. Journal of Neuro-Oncology, 2012, 109, 53-62.	2.9	26
78	"Soggy sand―electrolyte based on COOH-functionalized silica nanoparticles for dye-sensitized solar cells. Electrochemistry Communications, 2012, 16, 10-13.	4.7	26
79	Preparation of CdS-CoSx photocatalysts and their photocatalytic and photoelectrochemical characteristics for hydrogen production. International Journal of Hydrogen Energy, 2019, 44, 27795-27805.	7.1	26
80	Necroptotic virotherapy of oncolytic alphavirus M1 cooperated with Doxorubicin displays promising therapeutic efficacy in TNBC. Oncogene, 2021, 40, 4783-4795.	5.9	26
81	Enhanced conversion efficiency of dye-sensitized titanium dioxide solar cells by Ca-doping. Journal of Alloys and Compounds, 2013, 548, 161-165.	5.5	25
82	TiO2 flowers and spheres for ionic liquid electrolytes based dye-sensitized solar cells. Electrochimica Acta, 2013, 87, 629-636.	5.2	25
83	Computer simulations of light scattering and mass transport of dye-sensitized nanocrystalline solar cells. Journal of Electroanalytical Chemistry, 2006, 588, 51-58.	3.8	23
84	A classical PKA inhibitor increases the oncolytic effect of M1 virus via activation of exchange protein directly activated by cAMP 1. Oncotarget, 2016, 7, 48443-48455.	1.8	23
85	An Increase in Conversion Efficiency of Dye-Sensitized Solar Cells using Bamboo-Type TiO2 Nanotube Arrays. Electrochimica Acta, 2014, 116, 26-30.	5.2	22
86	Novel polymer electrolytes containing chemically crosslinked gelators for dye-sensitized solar cells. Polymers for Advanced Technologies, 2006, 17, 512-517.	3.2	21
87	Synthesis of pyridine derivatives and their influence as additives on the photocurrent of dye-sensitized solar cells. Journal of Applied Electrochemistry, 2009, 39, 147-154.	2.9	21
88	Mono-ion transport electrolyte based on ionic liquid polymer for all-solid-state dye-sensitized solar cells. Solar Energy, 2012, 86, 1546-1551.	6.1	21
89	Plastic dye-sensitized solar cells with enhanced performance prepared from a printable TiO2 paste. Electrochemistry Communications, 2013, 34, 254-257.	4.7	21
90	Transcriptional upregulation of microtubule-associated protein 2 is involved in the protein kinase A-induced decrease in the invasiveness of glioma cells. Neuro-Oncology, 2015, 17, 1578-1588.	1.2	21

#	Article	IF	CITATIONS
91	Inhibition of the mevalonate pathway enhances cancer cell oncolysis mediated by M1 virus. Nature Communications, 2018, 9, 1524.	12.8	21
92	The effect mechanism of 4-ethoxy-2-methylpyridine as an electrolyte additive on the performance of dye-sensitized solar cell. Colloids and Surfaces A: Physicochemical and Engineering Aspects, 2008, 326, 42-47.	4.7	20
93	In situ quaterizable oligo-organophosphazene electrolyte with modified nanocomposite SiO2 for all-solid-state dye-sensitized solar cell. Electrochimica Acta, 2009, 54, 4186-4191.	5.2	19
94	PEO-imidazole ionic liquid-based electrolyte and the influence of NMBI on dye-sensitized solar cells. Electrochimica Acta, 2011, 56, 6271-6276.	5.2	19
95	Wavelet analysis of the surface morphologic of nanocrystalline TiO2 thin films. Surface Science, 2005, 579, 37-46.	1.9	17
96	A novel thixotropic and ionic liquid-based gel electrolyte for efficient dye-sensitized solar cells. Electrochimica Acta, 2012, 68, 235-239.	5.2	17
97	CCGD-ESCC: A Comprehensive Database for Genetic Variants Associated with Esophageal Squamous Cell Carcinoma in Chinese Population. Genomics, Proteomics and Bioinformatics, 2018, 16, 262-268.	6.9	17
98	Systematic Characterization of the Biodistribution of the Oncolytic Virus M1. Human Gene Therapy, 2020, 31, 1203-1213.	2.7	17
99	Identification of the receptor of oncolytic virus M1 as a therapeutic predictor for multiple solid tumors. Signal Transduction and Targeted Therapy, 2022, 7, 100.	17.1	17
100	Experimental Research on Seafloor Mapping and Vertical Deformation Monitoring for Gas Hydrate Zone Using Nine-Axis MEMS Sensor Tapes. IEEE Journal of Oceanic Engineering, 2019, 44, 1090-1101.	3.8	16
101	Cyclometalated ruthenium( <scp>ii</scp> ) complexes with bis(benzimidazolyl)benzene for dye-sensitized solar cells. RSC Advances, 2015, 5, 90001-90009.	3.6	15
102	Dual Functional CuO <sub>1–<i>x</i></sub> Clusters for Enhanced Photocatalytic Activity and Stability of a Pt Cocatalyst in an Overall Water-Splitting Reaction. ACS Sustainable Chemistry and Engineering, 2018, 6, 17340-17351.	6.7	15
103	Genotype imputation for Han Chinese population using Haplotype Reference Consortium as reference. Human Genetics, 2018, 137, 431-436.	3.8	15
104	Characterization of TiO2 nanocrystalline thin film by scanning tunneling microscopy and scanning tunneling spectroscopy. Applied Surface Science, 1999, 143, 169-173.	6.1	14
105	Electrochemical impedance analysis of nanoporous TiO2 electrode at low bias potential. Chinese Chemical Letters, 2010, 21, 959-962.	9.0	13
106	Pre-synthesized monodisperse PbS quantum dots sensitized solar cells. Electrochimica Acta, 2014, 144, 71-75.	5.2	13
107	Selective Antagonism of Bcl-xL Potentiates M1 Oncolysis by Enhancing Mitochondrial Apoptosis. Human Gene Therapy, 2018, 29, 950-961.	2.7	13
108	Negative regulation of miRâ€1275 by H3K27me3 is critical for glial induction of glioblastoma cells. Molecular Oncology, 2019, 13, 1589-1604.	4.6	13

#	Article	IF	CITATIONS
109	Novel counter electrodes based on NiP-plated glass and Ti plate substrate for dye-sensitized solar cells. Journal of Materials Science, 2007, 42, 5281-5285.	3.7	12
110	Zinc-finger antiviral protein acts as a tumor suppressor in colorectal cancer. Oncogene, 2020, 39, 5995-6008.	5.9	12
111	Preparation of porous nanocrystalline TiO2 electrode by screen-printing technique. Science Bulletin, 2007, 52, 2481-2485.	1.7	11
112	Polymer–metal complex as gel electrolyte for quasi-solid-state dye-sensitized solar cells. Electrochimica Acta, 2011, 56, 1605-1610.	5.2	11
113	Photocatalytic activity enhancement of TiO <sub>2</sub> porous thin film due to homogeneous surface modification of RuO <sub>2</sub> . Journal of Materials Research, 2011, 26, 1532-1538.	2.6	11
114	Deficiency of the IRE1α-Autophagy Axis Enhances the Antitumor Effects of the Oncolytic Virus M1. Journal of Virology, 2018, 92, .	3.4	11
115	Real-Time Visualization and Quantification of Oncolytic M1 Virus <i>In Vitro</i> and <i>In Vivo</i> . Human Gene Therapy, 2021, 32, 158-165.	2.7	11
116	Quasi-solid state dye-sensitized solar cells based on pyridine or imidazole containing copolymer chemically crosslinked gel electrolytes. Science Bulletin, 2007, 52, 2320-2325.	1.7	10
117	Fluorescence and sensitization performance of phenylene-vinylene-substituted polythiophene. Science Bulletin, 2009, 54, 1669-1676.	9.0	10
118	Performance characteristics of dye-sensitized solar cells with counter electrode based on NiP-plated glass and titanium plate. Current Applied Physics, 2009, 9, 1005-1008.	2.4	10
119	Low temperature fabrication of flexible carbon counter electrode on ITO-PEN for dye-sensitized solar cells. Chinese Chemical Letters, 2010, 21, 1137-1140.	9.0	10
120	Facile fabrication of highly porous photoanode at low temperature for all-plastic dye-sensitized solar cells with quasi-solid state electrolyte. Journal of Power Sources, 2014, 271, 8-15.	7.8	10
121	Effects of Ga doping and hollow structure on the band-structures and photovoltaic properties of SnO <sub>2</sub> photoanode dye-sensitized solar cells. RSC Advances, 2015, 5, 93765-93772.	3.6	10
122	Rheological behavior for laponite and bentonite suspensions in shear flow. AIP Advances, 2019, 9, 125233.	1.3	9
123	Characterization of nanocrystalline porous CdSe thin films by electrolyte electroabsorption spectroscopy. Thin Solid Films, 2005, 479, 188-192.	1.8	8
124	A new type quasi-solid state electrolyte for dye-sensitized solar cells. Science Bulletin, 2006, 51, 1551-1556.	1.7	8
125	Novel chemically cross-linked solid state electrolyte for dye-sensitized solar cells. Electrochimica Acta, 2010, 55, 5803-5807.	5.2	8
126	An ionic liquidâ€based polymer with Ï€â€stacked structure as allâ€solidâ€state electrolyte for efficient dyeâ€sensitized solar cells. Journal of Applied Polymer Science, 2013, 127, 2574-2580.	2.6	8

#	Article	IF	CITATIONS
127	Preparation of monodispersed PbS quantum dots on nanoporous semiconductor thin film by two-phase method. Journal of Alloys and Compounds, 2014, 595, 51-54.	5.5	8
128	Suppression of CCDC6 sensitizes tumor to oncolytic virus M1. Neoplasia, 2021, 23, 158-168.	5.3	8
129	Photoelectrochemical studies of H2 evolution in aqueous methanol solution photocatalysed by Q-ZnS particles. Journal of Photochemistry and Photobiology A: Chemistry, 1999, 125, 135-138.	3.9	7
130	Double dye cubic-sensitized solar cell based on Förster resonant energy transfer. RSC Advances, 2015, 5, 10026-10032.	3.6	7
131	Controlled optical properties of water-soluble CdTe nanocrystals via anion exchange. Journal of Colloid and Interface Science, 2016, 463, 69-74.	9.4	7
132	Tumors driven by <i>RAS</i> signaling harbor a natural vulnerability to oncolytic virus M1. Molecular Oncology, 2020, 14, 3153-3168.	4.6	7
133	Air bubbles play a role in shear thinning of non-colloidal suspensions. Physics of Fluids, 2021, 33, .	4.0	7
134	Surface roughness effect on the shear thinning of non-colloidal suspensions. Physics of Fluids, 2021, 33, .	4.0	7
135	Rheology of bentonite dispersions: Role of ionic strength and solid content. Applied Clay Science, 2021, 214, 106275.	5.2	7
136	Local conductivity study of TiO2 electrodes by atomic force microscopy. Surface and Interface Analysis, 2001, 32, 125-129.	1.8	6
137	The effect of oligo-organosiloxane on poly(ethylene oxide) electrolyte system for solid dye sensitized solar cells. Electrochimica Acta, 2013, 89, 29-34.	5.2	6
138	Study on the Motion Stability of the Autonomous Underwater Helicopter. Journal of Marine Science and Engineering, 2022, 10, 60.	2.6	6
139	Efficiency enhancement of solidâ€state dye sensitized solar cell by <i>in situ</i> deposition of Cul. Surface and Interface Analysis, 2008, 40, 1393-1396.	1.8	5
140	Performances improvement of eosin Y sensitized solar cells by modifying TiO2 electrode with silane-coupling reagent. Science Bulletin, 2009, 54, 2633-2640.	9.0	5
141	Molecular organic conductors with triiodide/hole dual channels as efficient electrolytes for solid-state dye sensitized solar cells. RSC Advances, 2012, 2, 5550.	3.6	5
142	Lonidamine potentiates the oncolytic efficiency of M1 virus independent of hexokinase 2 but via inhibition of antiviral immunity. Cancer Cell International, 2020, 20, 532.	4.1	5
143	Studies on the interfacial charge transfer processes of nanocrystalline CdSe thin film electrodes by intensity modulated photocurrent spectroscopy. Science in China Series B: Chemistry, 2000, 43, 443-449.	0.8	4
144	Dye-sensitized solid-state solar cells fabricated by screen-printed TiO2 thin film with addition of polystyrene balls. Chinese Chemical Letters, 2008, 19, 1004-1007.	9.0	4

#	Article	IF	CITATIONS
145	Polymer electrolyte using <i>in situ</i> quanternization for all solidâ€state dyeâ€sensitized solar cells. Polymers for Advanced Technologies, 2009, 20, 519-523.	3.2	4
146	Electrodeposition of SnO2 nanocrystalline thin film using butyl-rhodamine B as a structure-directing agent. Chinese Chemical Letters, 2010, 21, 1505-1508.	9.0	4
147	Enhanced Performance of Dye-Sensitized Solar Cells By Tuning the Structure of the Photoanode Film. Electrochimica Acta, 2014, 145, 286-290.	5.2	4
148	Visualization of the Oncolytic Alphavirus M1 Life Cycle in Cancer Cells. Virologica Sinica, 2021, 36, 655-666.	3.0	4
149	Light scattering characteristic of TiO2 nanocrystalline porous films. Science Bulletin, 2003, 48, 856.	1.7	4
150	High conversion efficiency of pristine TiO2 nanotube arrays based dye-sensitized solar cells. Science Bulletin, 2012, 57, 864-868.	1.7	3
151	Insulation Degradation Analysis Due to Thermo-Mechanical Stress in Deep-Sea Oil-Filled Motors. Energies, 2022, 15, 3963.	3.1	3
152	Influence of chemical treatments on the photoinduced charge carrier kinetics of nanocrystalline porous TiO2 films. Journal of Photochemistry and Photobiology A: Chemistry, 2003, 159, 41-45.	3.9	2
153	Femtosecond Time-Resolved Near-Field Spectroscopy of CdSe Nanocluster Films. Chinese Physics Letters, 1999, 16, 683-685.	3.3	1
154	Preparation of nano-Pt-modified electrode and its electrocatalytic activity investigation. Materials Chemistry and Physics, 2006, 97, 261-266.	4.0	1
155	Overcoming resistance to oncolytic virus M1 by targeting PI3K-γ in tumor associated myeloid cells. Molecular Therapy, 2022, , .	8.2	1
156	Scanned laser spot photocurrent response studies of surface modifications of CdSe thin film electrodes. Applied Surface Science, 1995, 90, 321-324.	6.1	0
157	Zinc-Doping in TiO <sub>2 </sub> Films to Enhance Photovoltaic Performance of Dye-Sensitized Solar Cells. Applied Mechanics and Materials, 2011, 66-68, 224-228.	0.2	0
158	Effect of TiO2 nanotubes lateral spacing on photovoltaic properties of dye-sensitized solar cells. Science Bulletin, 2014, 59, 4735-4740.	1.7	0